From Buncefield to Tunguska: Hazard and Disaster Modelling at the University of Southampton

N.J. Bailey, J.S. Bevington, H.G. Lewis, G.G. Swinerd[1], P.M. Atkinson[2], R. Crowther[3], D. Holland[4]

[1] School of Engineering Sciences, [2] School of Geography, University of Southampton, UK
[3]Rutherford Appleton Laboratory, UK
[4]Ordnance Survey Research, UK

ABSTRACT

The impact of a Near Earth Object (NEO) on the Earth represents a catastrophic, multi-hazard, natural disaster. One in ten detected NEOs have significantly non-zero Earth impact probabilities and it is probable that within two decades the international community will face critical decisions on its response to a possible NEO impact. However, improved modelling and simulation tools are required to support the development of a science-based policy to address the NEO impact risk. Research projects ongoing at the University of Southampton, presented here, target different aspects of this modelling issue.

Firstly, a novel change-detection model is being developed to extract information about the type and scale of damage done to buildings as a result of natural or technological disasters. The automatic provision of this information is of considerable benefit to responders and policy-makers alike, as comparison with damage levels established for other events and hazards allows a consistent and appropriate policy solution to be established. The object detection phase of the model has been applied to remotely sensed imagery of the Buncefield Oil Depot, UK, and is presented. Secondly, using the University's *NEOimpactor* tool, a study has been conducted to quantify the risk to individual nations, in terms of the human and economic consequences, from an impacting asteroid. Results show developing countries and their more industrialised neighbours are equally at risk, with considerable loss of life and property over a broad area.

1. INTRODUCTION

Natural and anthropogenic disasters can take many forms from localised effects of tornados or building collapse, to continental or global scale events, such as tsunamis. Hundreds of millions of people globally are at risk of such disasters and as a result, researchers and aid agencies have adopted remote sensing technologies in order to assess damage and monitor rescue and recovery efforts in instances such as the 2004 Indian Ocean tsunami (Miura *et al*., 2005) and the September 11th 2001 terrorist attacks (Huyck and Adams, 2002). Such hazards are, however, small in comparison to the potential devastation from the impact of even a modest sized asteroid. A Near Earth Object (NEO) is an asteroid or comet whose orbit brings it close to the Earth. These objects vary in size and composition, from small, rocky asteroids several metres in diameter to large, icy comets many kilometers across. Due to their high relative speeds with respect to the Earth and large mass, NEOs typically have extremely high kinetic energies, which on impact can be equivalent to the detonation of many nuclear weapons. Impact generated effects (IGEs) include an atmospheric pressure blast wave, thermal radiation from the expanding fireball, the ground transmitted seismic shock energy and the distribution of ejecta excavated from the impact site. Ocean impacts are characterised by the generation of a tsunami which propagates from the impact site to affect the surrounding coastlines. Consequently, the impact of a NEO on the Earth represents a catastrophic, multi-hazard, natural disaster.

The International Spaceguard survey is developing a catalogue of all NEOs larger than one kilometre in diameter and work is progressing on cataloguing smaller objects (Stokes *et al*., 2007). To date, nearly 4,800 NEOs larger than one kilometre have been catalogued and approximately 400 objects have been detected with significantly non-zero Earth impact probabilities. Near Earth objects smaller than one kilometre remain predominantly undetected but exist in far greater numbers and impact the Earth more frequently. Due to advances in detection and mitigation capability it is probable that within two decades the international community will face critical decisions on its response to a possible NEO impact.

Several roadblocks to the development of a science-based policy to address the NEO impact hazard exist. These include the need to identify suitable damage scales and indices, comparable to existing scales for wind and flood damage, for example, in order to ensure that an appropriate and consistent response can be established. In addition, improved modelling tools are required to simulate impact response, in order to understand the evolution of an impact disaster and the demands on response agencies, communication systems and transport infrastructure. Of particular importance, is the need to capture the response of all stakeholders, including local and national governments, military organisations, disaster responders, members of the press, and the civilians at risk. Present approaches tend to focus on a particular aspect of the impact process,

from atmospheric entry to impact mechanics, with no modelling of the overall socioeconomic consequences in an integrated manner.

Independent research projects ongoing at the University of Southampton target some aspects of these roadblocks. Firstly, a novel change-detection model is being developed to extract information about the type and scale of damage done to buildings as a result of natural or technological disasters. Many existing methods for damage detection are based on "image differencing" where each pixel in images captured before and after an event are assigned to a class and the classified images are compared (Singh, 1989). Other techniques rely heavily on non-automated visual comparison of images (Adams *et al.,* 2004). Whilst not directed specifically at the NEO hazard, the rapid provision of this information using a new, automatic method is of considerable benefit to responders and policy-makers dealing with the consequences of a NEO impact and natural disasters in general. Secondly, knowledge drawn from the impact model literature has been used to develop a new global impact simulator, the focus of which is the consequences for human populations and the associated infrastructure damage. The various IGEs are modeled together to simulate the result of a NEO impact, although each effect could be modeled independently to simulate other natural hazards such as earthquakes, tsunami, and hail storms.

2. CHANGE DETECTION MODEL

The model described in this section aims to detect and quantify changes in building infrastructure extracted from optical imagery. Figure 1 shows the conceptual model adopted for this approach, consisting of a module for object detection and one for object comparison.

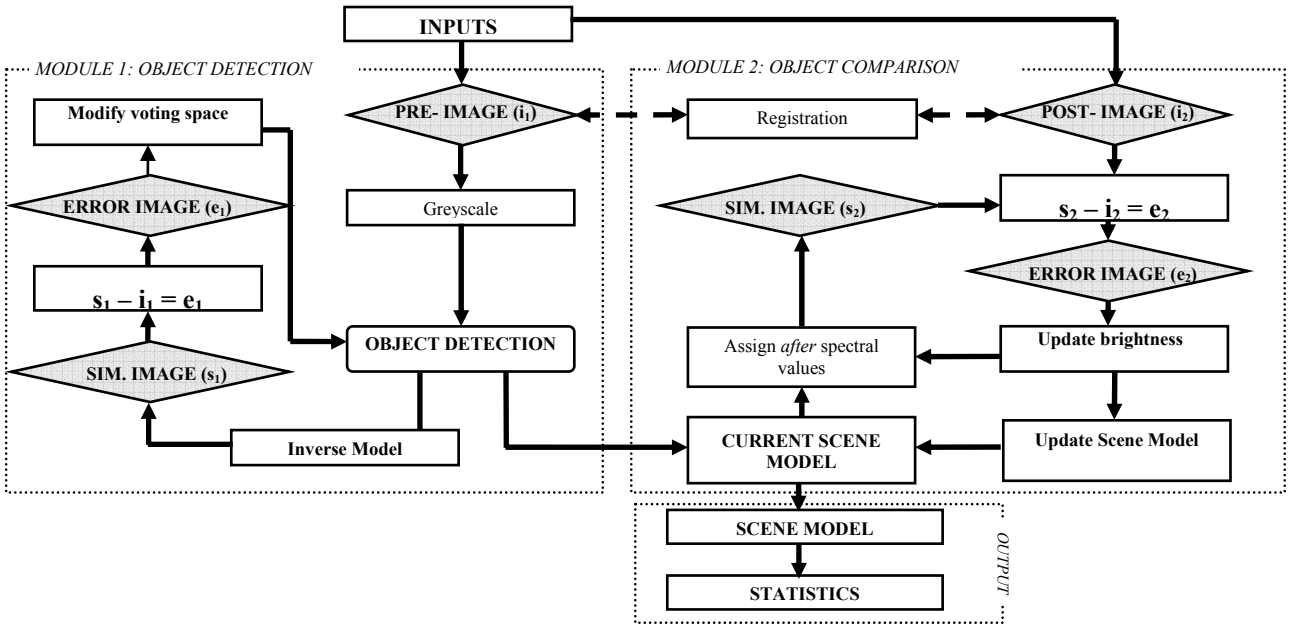

Figure 1. Workflow of change-detection conceptual Model

A pair of fine spatial resolution, remotely-sensed, optical images (captured before and after the change event) are used as the input to the model. An object detection algorithm is applied to the pre-event image to identify building outlines, which are extracted as contiguous objects from this image space into a scene space. The scene space is a simplified raster or vector representation of the real world. Subsequently, a forward model is used to create a simulated image of the objects in the scene, by assigning characteristic radiometric brightness values to each object and the background. The brightness values of this simulated image are then compared to real-world data from the pre-event remotely-sensed image (the *before* image) and a brightness error image is generated. Finally, the error image is used to adapt the object detection algorithm (inverse modelling) so as to improve the identification of buildings. The forward and inverse modelling approach is applied in an iterative manner, with changes made to the object detection algorithm such that the brightness errors are minimised and the scene model becomes the best fit to the pre-event image.

The object comparison module is the main change detection component of the model, through which object change can be monitored and measured. The key inputs are a geo-registered optical image of the change-affected area (the *after* image) as well as a raster scene model of objects defined in the object detection module. Alternatively, this scene model can be

generated by rasterising an existing geo-registered vector dataset of target objects, providing the *before* geometric boundaries of the objects in a scene model. In this phase, the brightness properties of these objects are compared iteratively with the brightness values of the image captured *after* the change event and an error image produced based on these differences. A forward model iteratively updates the spectral and geometric properties of the objects in the scene model using a shape morphing technique with the error image informing further iterations, resulting in the reduction of error in the scene. The time-history of spectral and geometric change vectors are stored automatically with object-based statistics quantifying the changes in objects between the images. The process continues until convergence is achieved at an appropriate level of error. Additional algorithms can be implemented to improve performance of any energy minimisation technique to avoid convergence at local energy minima in favour of global minima.

2.1 Application to the 2005 Buncefield Oil Depot Fire

Implementation of the object detection phase is discussed briefly here, but is described fully in Bevington *et al.* (2007). Aerial imagery of the Buncefield Oil Depot, UK, which was extensively damaged in a 2005 fire, was acquired in 1999 with spatial resolution of 50 cm. An advanced Hough Transform (HT) circle detection algorithm was applied to a smoothed 8-bit greyscale 292 × 292 pixel subset of the image containing three oil tanks. The HT algorithm generated an accumulator space showing the probability of a pixel lying on the edge of a circle. These circles represented the objects of interest in the scene model. The forward model assigned a uniform brightness value of 240 (obtained from the mean spectral signature of the top of an oil drum) to each circle detected and 160 to the background. The error image was created by subtracting the pixel brightness values of the input image from those in the simulated image, standardised and combined with the initial accumulator values to modify the accumulator space. A nominal value was introduced to reduce the impact of the error image on the accumulator space as described by Bevington *et al.* (2007). These processes were repeated iteratively, for 200 iterations, updating the accumulator space based on the modified accumulator score from the previous iteration (Figure 2). Statistics were generated to gauge the relationship between the simulated image and the input image (Figure 3).

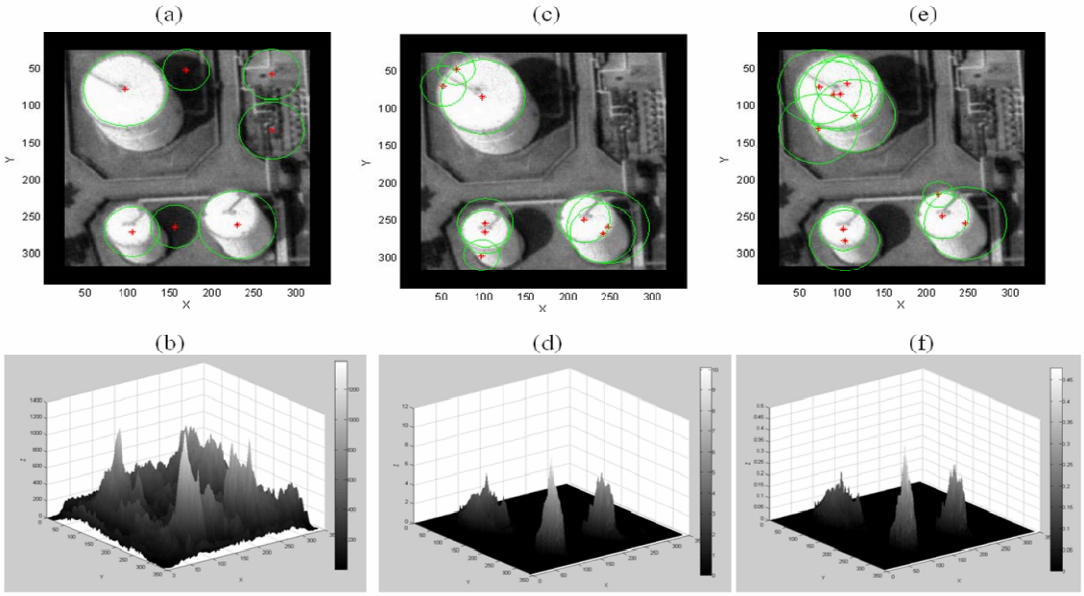

Figure 2. Circle detection and accumulator values at 1 (a & b), 50 (c &d) and 100 (e & f) iterations

The first iteration of the HT identified seven circles; three approximating the tops of the oil tanks in the image. The initial accumulator showed some evidence (typically < 800 votes) for circles in areas where tanks did not exist. However, a study of the modified accumulator spaces seen in later iterations (Figure 2) revealed that votes in these areas were reduced to zero whilst voting peaks corresponding to tanks had been increased. The largest peaks (> 800 votes) remained at the centres of the oil tanks and erroneous circles, such as shadows, were dismissed in an automated and unsupervised fashion.

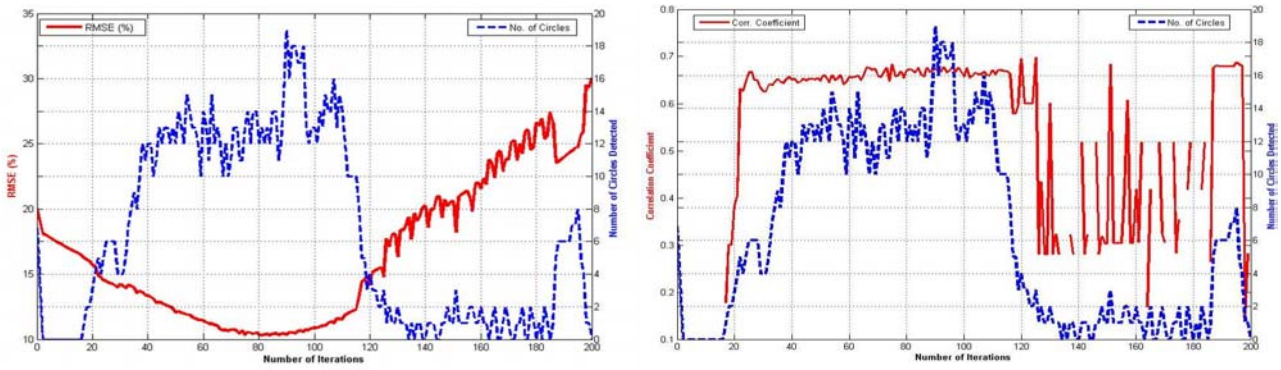

Figure 3. Number of circles detected with RMSE percentage (left), and correlation coefficient (right)

A dual contour approach (Gunn and Nixon, 1997) is being implemented for the geometric comparison phase of the model. Active contours, or snakes, were first described by Kass *et al.* (1998), as a method of delineating image features by evolving a polygon from an initial starting point to completely enclose the external or internal boundary of the target feature. The dual contour method combines two snakes that are initialised inside and outside the object of interest and evolve simultaneously; one expands while the other contracts until they converge along a target boundary. The dual approach reduces the number of times the model will settle on local minima, often characterised by areas with similar spectral properties as the target feature. Within the approach described in Figure 1, the scene model defined by the object detection module provides a-priori knowledge for active contour initialisation. However, for some events objects will exist in the post-event image that are not in the pre-event image, and vice versa. Consequently, it may be necessary to run a second object detection algorithm on the *after* image in order to capture newly created objects.

3. ASTEROID IMPACT MODEL

This work has focused on the development of a software tool, NEOimpactor, to quantify casualty and damage estimations following a NEO impact. There were a number of challenges to be overcome, notably the data handling requirement and the ability to manage the errors involved. In order to handle the large datasets, which contain information about the Earth, an internal database structure was developed to compile and store raw data and simulation results and to enable data retrieval. Land impacts of NEOs are characterised using the principle impact generated effect (IGE) models developed by Collins, Melosh & Marcus (2005) for the Arizona web-based Impact Effects program. Four principal IGEs are modelled – the blast wave, thermal radiation, the seismic shock energy and ejecta. These four effects are simulated simultaneously by the system and their consequences for the surrounding population and infrastructure mapped out. Ocean impacts are modelled by the generation of a tsunami. Cavitation of the ocean at the point of impact and subsequent tsunami generation has been modelled by Ward & Asphaug (2000). These models have been implemented together with a 'neural network' ocean path algorithm which enables the wave to diffract around coastlines (Bailey *et al*., 2007). The consequences for coastal communities from tsunami shoaling are calculated from the wave run-up and run-in capabilities.

The software architecture is built around a database model of the Earth, composed of a number of data layers, each of which contains a global data set. The resolution of the layer is defined by the datasets used and each layer can be pictured as a spherical overlay on a cellular globe. Three classes of layer are contained within the database: raw dataset layers obtained from remotely sensed imagery, IGE distribution data and human/infrastructure interaction layers. The database maintains a spherical coordinate system to minimise cartographic projection errors. The layered database structure enables each layer characteristic to be sampled for any location on Earth. Of particular importance are the population and infrastructure raw data layers. These are generated from global maps available on the internet. The population density data was sourced from the Socioeconomic Data and Applications Center[*] and a current global population figure was sourced from the CIA World Factbook[†]). No global infrastructure dataset was available and so an approximation was made by using a greyscale nighttime light pollution world map and making the assumption that regions of greater light pollution correlated to higher infrastructure density. Using a value for the global economic value (Jeidicke *et al*., 2003) the infrastructure value for each cell was inferred using a similar method to the population density.

Following simulation of the impact and prediction of the generated effects NEOimpactor performs an interaction algorithm between the IGE layers and the population and infrastructure data layers to calculate the percentage of inhabitants

[*] Socioeconomic Data and Applications Center [online] <http://sedac.ciesin.columbia.edu/gpw/>
[†] CIA World Factbook [online] <https://www.cia.gov/cia/publications/factbook>

and infrastructure in each cell that would be affected. This percentage is multiplied by the cell raw data values to generate a data layer of the casualties and damage generated. Data can be extracted from the database through cross referencing layers to derive comparison datasets. Of particular importance is the country layer allowing the sum casualty and damage per country to be calculated. Data layers can then be extracted as raster maps formatted in a Plate Carrée cylindrical projection.

3.1 Multi-impact Simulation

To investigate the general global threat posed by the NEO hazard the NEOimpactor system is run in a multi-impact mode. This simulates many impacts across the globe, generates a map of the relative consequences from each impact, so removing the error associated with the exact prediction of any single impact. In the multi-impact simulation, an asteroid is impacted into each cell of a global grid. The consequences (recorded as a total casualty and damage figure) resulting from each impact are recorded and used to shade the global map accordingly. The cell with the most casualties is shaded darkest and all other cells are shaded relative to this. The raw casualty and damage figures are recorded and summed across all impacts for each individual country in order to provide a ranking of the countries most affected. The resolution of the impact grid is 32 by 64 generating a total 2,048 impact simulations. The typical asteroid used for the simulation is a 100 m diameter, spherical body composed of a soft stone material (1500 kg/m^3) travelling at 12,000 m/s. Such an asteroid delivers 5.65×10^{16} joules of kinetic energy at the point of impact following atmospheric entry.

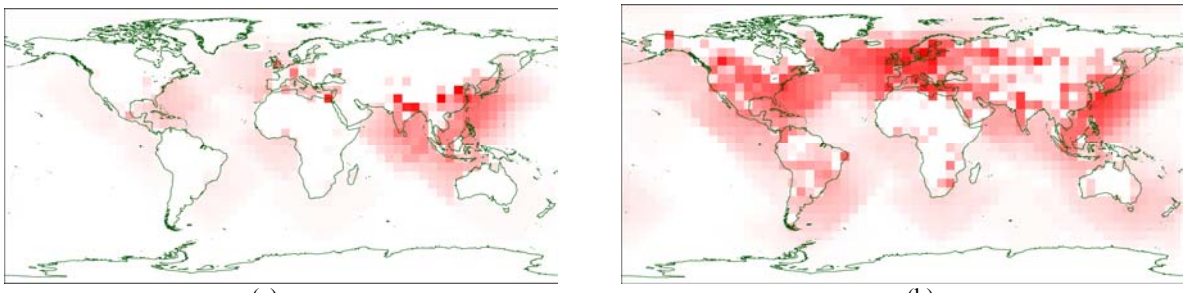

(a) (b)

Figure 4. Map of impact simulation with dark shading denoting (a) large casualty generation and (b) high infrastructure damage.

Figure 4a shows that ocean impacts present the most significant risk to human populations whilst land impact cells typically register relatively few casualties. Impact sites in the Indian and Pacific Ocean around Southeast Asia dominate the results with casualty figures exceeding 3 million in the worst scenario. A direct impact into Europe would have catastrophic consequences, although the smaller land area reduces the probability of such an event occurring. Southeast China, Indonesia, India and the Philippines record the most severe consequences in terms of casualties due to the densely populated coastal regions. While impacts into the central ocean regions still present a significant threat to coastal populations, the attenuation of the tsunami as it spreads acts to dissipate the energy and reduce the damage potential of the shoaling wave. The relatively low population density of inland Central Africa, Russia, Canada, Australia and South America reduces the overall impact hazard with the consequences for land impacts highly dependent on the exact impact location; while ocean impacts 20 km apart may generate only a negligible difference in the IGEs, on land such a separation could mean the difference between a direct strike on a city and an unpopulated area.

In Figure 4b, tsunami emanating from large areas of the ocean generate significant infrastructure loss. However, it is apparent that the relative consequences are spread more evenly across the Earth. The Northern hemisphere from the United States to Europe is at greatest risk, with ocean impacts in between able to cause damage on both coast lines. The historical development of large conurbations around ports results in a great array of infrastructure in easy reach of a tsunami wave. Infrastructure is critical to emergency aid procedures and significant destruction of any location, especially capital cities, will severely hamper the ability to provide aid and emergency relief.

Tables 1 and 2 present the top ten countries for casualty and damage respectively. Two thirds of all recorded casualties globally are attributed these ten countries and they account for nearly half the total damage recorded. A country's vulnerability is attributed to two main factors: the country's total population (or infrastructure wealth) and the ratio of its land area to coastline. Of the fifteen countries listed, eight are within the ten greatest populations, six in the ten wealthiest nations, and six in the top ten countries by land area. Notably none of the countries listed are land-locked and each apart from Nigeria possesses a significant length of coastline in proportion to their area.

Table 1. Percentage of global impact casualties.

	% of Global Casualty	% Summation
China	17.69	17.7
Indonesia	10.03	27.7
India	8.32	36.0
Japan	7.19	43.2
United States	6.31	49.5
Philippines	4.32	53.9
Italy	3.77	57.6
United Kingdom	3.28	60.9
Brazil	2.66	63.6
Nigeria	2.39	66.0

Table 2. Percentage of global infrastructure damage.

	% of Global Damage	% Summation
United States	9.85	9.9
China	7.69	17.5
Sweden	5.22	22.8
Canada	5.10	27.9
Japan	4.20	32.1
Mexico	4.18	36.2
Brazil	3.29	39.5
United Kingdom	3.24	42.8
Norway	3.09	45.8
Russia	3.07	48.9

4. CONCLUSIONS

As advances are made in the efforts to detect the population of NEOs and to mitigate the threat of an impact, it is likely that the international community will soon confront the prospect of deciding whether to take action and what action to take to avoid the consequences of a catastrophic natural disaster. In order to define an appropriate policy for addressing the NEO impact hazard, several roadblocks need to be overcome: placing the NEO impact hazard into context alongside other, more frequent natural disasters, and the robust understanding of the evolution of a NEO impact disaster. Whilst these issues are common to other natural disasters, the scale of the NEO impact generated effects is such that the whole globe may be affected and all nations are equally at risk. Results from ongoing research at the University of Southampton have shown that change-detection, applied to remotely-sensed imagery of natural and technological disasters, is capable of delivering information on damage over wide areas in an automatic fashion. Potentially, this will lead to a better understanding of the relative damage caused by a variety of disaster events. In addition, the University's NEOimpactor tool is providing policy-makers with the means to understand the socioeconomic consequences of a NEO impact. Results highlight those nations most at risk and, thus, those nations likely to be involved in multi-lateral cooperation to mitigate the NEO impact hazard.

Acknowledgments

The authors would like to recognise the financial support of the Engineering and Physical Sciences Research Council, Ordnance Survey and the British National Space Centre.

REFERENCES

Adams, B.J., Huyck, C.K., Mansouri, B., Eguchi, R.T. and Shinozuka, M., 2004. "Application of high-resolution optical satellite imagery for post-earthquake damage assessment: The 2003 Boumerdes (Algeria) and Bam (Iran) Earthquakes", State University of New York, Buffalo, NY, USA

Bailey, N.J., Swinerd, G.G., Morley, A.D., and Lewis, H.G., 2007, "Near Earth object impact simulation tool for supporting the NEO mitigation decision making process", Proceedings of the International Astronomical Union, vol. 2, Symposium S236, August 2006, Cambridge University Press, pp 477-486..

Bevington, J.S., Lewis, H.G. and Atkinson, P.M., 2007. "Quantitative Modelling of Unexpected Change Using Remotely-Sensed Imagery", *Proceedings of the 32nd International Symposium on Remote Sensing of Environment*, 25 - 29 June 2007, San Jose, Costa Rica.

Collins, G.S., Melosh, H.J., Marcus, R.A., "Earth Impact Effects Program: a Web-based Computer Program for Calculating the Regional Environmental Consequences of a Meteoroid Impact on Earth", Meteoritics & Planetary Science, Vol. 40, No. 6, 2005, pp. 817-840.

Gunn, S.R. and Nixon, M.S., 1997. A Robust Snake Implementation; A Dual Active Contour, *IEEE Transactions on Pattern Analysis and Machine Intelligence*, 19(1):63-68.

Huyck, C.K. and Adams, B.J., 2002. "Emergency response in the wake of the World Trade Center attack: The remote sensing perspective", State University of New York, Buffalo, NY, USA.

Jedicke, R., Morbidelli, A., Spahr, T., Petit, J.-M., Bottke, W.F., Jr., "Earth and Space-based NEO Survey Simulations: Prospects for Achieving the Spaceguard Goal", *Icarus*, Vol. 161, No. 1, 2003, pp. 17-33.

Kass, M., Witkin, A. and Terzopoulos, D., 1988. "Snakes: Active Contour Models", *International Journal of Computer Vision*, 1:321-331.

Miura, H., Wijeyewickrema, A.C. and Inoue, S., 2005. "Evaluation of tsunami damage in the eastern part of Sri Lanka due to the 2004 Sumatra earthquake using high-resolution satellite images", *Proceedings of the Third International Workshop on Remote Sensing for Post-Disaster Response*, 12-13 September 2005, Chiba, Japan.

Singh, A., 1989. "Review article: Digital change detection techniques using remotely-sensed data", *International Journal of Remote Sensing*, vol. 10(6) p.p. 989-1003.

Stokes, G. H., Yeomans, D. K., Bottke, W. F., Chesley, S. R., Evans, J. B., Gold, R. E., "Study to Determine the Feasibility of Extending the Search for Near-Earth Objects to Smaller Limiting Diameters", Report of the Near-Earth Object Science Definition Team, URL: http://neo.jpl.nasa.gov/neo/neoreport030825.pdf[cited 15 February 2007].

Ward, S.N., Asphaug, E., "Asteroid Impact Tsunami: a Probabilistic Hazard Assessment", *Icarus*, Vol. 145, No. 1, 2000, pp. 64-78.